Nuclear Physics **A412** (1984) 534–550

FRAGMENTATION OF RELATIVISTIC ^{56}Fe NUCLEI IN EMULSION

G.M. CHERNOV, K.G. GULAMOV*, U.G. GULYAMOV, V.Sh. NAVOTNY*, N.V. PETROV and L.N. SVECHNIKOVA*

Institute of Nuclear Physics, Uzbek Academy of Sciences, Ulugbek, Tashkent 702132, USSR

and

B. JAKOBSSON, A. OSKARSSON and I. OTTERLUND

University of Lund, Sölvegatan 14, S-223 62 Lund, Sweden

Received 30 May 1983
(Revised 26 August 1983)

Abstract: Experimental data on general characteristics of projectile fragments in inelastic interactions of relativistic ^{56}Fe nuclei in emulsion (multiplicities, transverse momentum distributions, azimuthal correlations) are presented and discussed. A strong dependence on the mass number of the projectile nucleus is observed for the transverse momenta of the emitted projectile fragments. These fragments exhibit an azimuthal asymmetry caused by the transverse motion of the fragmenting residue, but it is shown that this motion can be responsible only for a part of the increase in the average transverse momentum of the fragments with increasing mass of the projectile.

E | NUCLEAR REACTIONS H, C, N, O, Ag, Br(^{56}Fe, X), $E = 1700$ MeV/nucleon; measured σ(projectile fragment, θ), projectile fragment multiplicities, transverse distributions. Nuclear emulsions.

1. Introduction

Fragmentation of relativistic projectile nuclei is in general a relatively well isolated process in the complex scheme of high-energy reactions between multibaryon systems. Experimental knowledge of this process is essential for studies of how the heavy cosmic-ray spectrum is changed during transport through the universe.

The first experimental information about fragmentation of nuclei was in fact obtained in experiments with cosmic-ray particles [see e.g. refs. [1,2])]. Acceleration of heavy ions up to relativistic energies at Berkeley and Dubna gave an opportunity of more detailed studies of this phenomenon and a number of papers, both experimental and theoretical, have been published during the last decade on the fragmentation of light nuclei ($A_P \leq 16$) [ref. [3]), and references therein].

Fragmentation of accelerated iron nuclei have been considered more recently in refs. [3,4]). The experimental data on the yield of projectile fragments with charges

* Permanent address: S.V. Starodubtsev Physical Technical Institute, Tashkent 700084, USSR.

$Z \geq 13$ were presented in ref. [3]). In ref. [4]) it was experimentally observed that in inelastic collisions of ^{56}Fe nuclei in emulsion the angular distribution of "spectator" α-particles became considerably wider than in analogous interactions of ^{16}O nuclei.

In the present paper we report on experimental data for fragmentation of ^{56}Fe nuclei in emulsion at an incident momentum of 2.5 GeV/c per nucleon. We discuss the yield of projectile fragments with charges $Z = 1$–8 and $Z \geq 9$ from collisions with light and heavy emulsion nuclei. The factorization of fragmentation cross sections, transverse momentum distributions and correlations between projectile fragments in the azimuthal plane are discussed after comparison with data from ^{12}C- and ^{14}N-induced reactions.

2. Experimental material

The experiment has been performed in a stack of Ilford G5 nuclear emulsions exposed at the LBL (Berkeley) to a beam of ^{56}Fe ions with kinetic energy 1.9 GeV per nucleon. The ionization losses of the primary nuclei in emulsion before the interactions reduce the average incident momentum for Fe-Em collisions to 2.5 ± 0.1 GeV/c per nucleon ($\langle E_{\text{kin}} \rangle = 1.7 \pm 0.1$ GeV per nucleon).

Over the total length of 109.8 m of scanned primary tracks we have registered 1308 interactions which corresponds to the mean free path of ^{56}Fe nuclei in emulsion equal to 8.4 ± 0.2 cm. Events without charged secondary particles, production of energetic δ-electrons and e^+e^- pairs were not registered. Events close to the surface and glass were removed. The remaining 980 Fe-Em interactions were used for further analysis. Charged secondaries in these events were classified into the following types: "black" particles (b-particles) with a range in emulsion $l \leq 3$ mm ($E_{\text{proton}} \leq 26$ MeV), "grey" particles (g-particles) with $l \geq 3$ mm and velocity $\beta = v/c < 0.7$ ($26 < E_{\text{proton}} < 375$ MeV), shower particles (s-particles) – singly charged particles with $\beta > 0.7$, and "noninteracting" fragments of the projectile nucleus (f-particles) with charge $Z \geq 2$. For b- and g-particles together one uses the term "heavy-track-producing particles". The polar, θ, and azimuthal, ϕ, emission angles were measured for all charged secondary particles. The errors in the angles have been estimated from repeated measurements on tracks from real events and on tracks from pseudo-events. In the latter case we initiated a one-prong event by choosing an arbitrary point on a straight track as the centre of the event. In this pseudo-event there is one prong from the "incident" particle and one forward prong from the "emitted" particle. We measured the angle of this forward prong on tracks with different Z. The uncertainties in angles on relativistic tracks with $\theta < 3°$ are $\Delta\theta \approx \pm 0.1°$.

In the present paper we discuss characteristics of noninteracting (spectator) fragments from the projectile iron nuclei (hereafter called fragments). They include all f-particles and a part of the s-particles.

Selection of f-particles in nuclear emulsions can easily be performed since these tracks are characterized by high ionization which, in contrast to b- and g-particles,

does not change over large distances (several cm). Furthermore they do not reveal noticeable multiple scatterings. The charges of f-particles have been determined by measurements of the number of gaps and δ-electrons on a track length of more than 1 cm. This method allows charge identification in the range $2 \leqslant Z \leqslant 8$ with an accuracy which is better than ± 1. For $Z \geqslant 9$ the error in the charge measurements is of the order of unity or larger and therefore fragments with $Z \geqslant 9$ will be considered subsequently as one subgroup.

It is more difficult to identify singly charged projectile fragments. For this purpose we use a statistical method based on the comparison of angular distributions of s-particles produced in nucleus–nucleus and proton–nucleus collisions at the same energy per nucleon. We assume that the angular distribution of singly charged projectile fragments in the laboratory frame can be written as

$$\frac{\mathrm{d}N}{\mathrm{d}\cos\theta} \sim A_F^2 p_0^2 \cos\theta \exp\left[-A_F^2 p_0^2 (1-\cos^2\theta)/2\sigma^2\right], \tag{1}$$

where A_F is the mass number of a fragment and p_0 is the incident momentum per nucleon. Formula (1) corresponds to a transverse momentum distribution of the type

$$\frac{\mathrm{d}N}{\mathrm{d}p_\perp} = \frac{p_\perp}{\sigma^2} \exp\left(-p_\perp^2/2\sigma^2\right). \tag{2}$$

The experimental data on p-A collisions show [5]) that the angular distribution of "produced" s-particles at small emission angles θ can be written as

$$\frac{\mathrm{d}N}{\mathrm{d}\cos\theta} = \text{const.} \tag{3}$$

We have fitted the angular distribution of s-particles in Fe-Em interactions to a sum of the distributions (1) and (3) (see fig. 1). This procedure allows one to determine the angle θ_0 which is meant to separate s-particles of fragmentation type

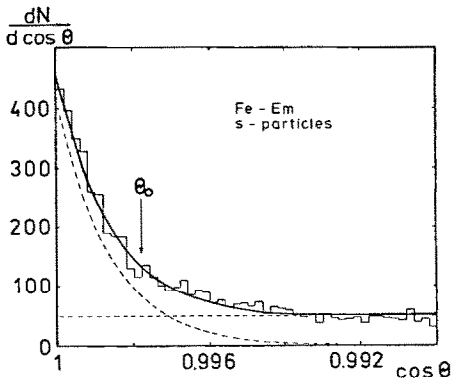

Fig. 1. Angular distributions of s-particles in Fe-Em interactions. The solid curve represents the fit to the data ($x^2/\mathrm{DOF} = 1.2$) by the sum of distributions (1) and (2) (dashed lines).

($\theta < \theta_0$) and s-particles produced in more violent processes ($\theta > \theta_0$). The value of θ_0 is chosen in such a way that the number of fragments with $\theta > \theta_0$ is equal to the number of "produced" s-particles having $\theta < \theta_0$. We have found that the contribution of "produced" relativistic particles in the region $\theta < \theta_0$ is approximately 12% of all s-particles here. The use of a "limiting" angle θ_0 is quite reasonable when estimating average multiplicities of singly charged fragments in different ensembles of Fe-Em interactions. We found that the described procedure of fragment separation is weakly (if at all) dependent on the mass of the target nucleus. Of course when estimating $p_\perp$ distributions for singly charged fragments the tails of the θ-distributions should be taken into account. This has been done under additional assumptions about the contributions of protons, deuterons and tritons, based on well-known experimental data on the fragmentation of nuclei obtained in spectrometer experiments [6]).

We have separated the Fe-Em interactions into ensembles of collisions with hydrogen (Fe-H, $A_T = 1$), light (Fe-CNO, $\langle A_T \rangle = 14$) and heavy (Fe-AgBr, $\langle A_T \rangle = 94$) emulsion nuclei. Fe-H collisions were selected using constraints on n_h, the multiplicity of heavily ionizing particles, kinematics of the event and features of p-Em collisions in the antilaboratory frame, based on the experimental data on proton–nucleus interactions. The detailed description of this procedure will be published elsewhere. From 179 events satisfying the necessary criteria for Fe-H interactions in emulsion, we have excluded 45 two-prong stars, one prong being the projectile with unchanged ionization and the second one being the black track of a recoil proton, satisfying the kinematics of elastic Fe-p scattering. The remaining events with $n_h \leq 8$ (events with $n_h > 8$ are Fe-AgBr collisions) were divided into Fe-CNO and Fe-AgBr interactions following the method described for p-A interactions in ref. [7]). Below we analyse 134 Fe-H, 319 Fe-CNO and 482 Fe-AgBr inelastic interactions.

It should be noted that when analysing the data we consider in all cases the uncertainties in identification of the target mass and in the separation of singly charged fragments. When these problems are not specially discussed, they are small and cannot change any conclusion.

3. Multiplicity of fragments

In table 1 we present data on the average multiplicity of fragments with different charge, Z, in interactions of iron nuclei in emulsion. Only statistical errors are quoted. The possible systematic errors due to the above-mentioned uncertainties in the identification are estimated to be of the same order (for $Z = 1$) or smaller (for $Z \geq 2$ fragments) than the statistical ones. Measurements of Fe fragmentation ($13 \leq Z_F \leq 25$) have been performed by Westfall *et al.* [3]). A parametrisation of the existing data in the spirit of limiting fragmentation results in the multiplicities $\langle n_{9-25} \rangle = 0.9$ and $\langle n_{9-25} \rangle = 0.7$ for fragments in the charge group $9 \leq Z_F \leq 25$ for ^{56}Fe-H and ^{56}Fe-CNO reactions, respectively. These multiplicities are similar to

TABLE 1

Multiplicities of projectile fragments in interactions of relativistic ^{56}Fe nuclei in emulsion

Charge of fragments Z	$\langle n_Z \rangle$			
	Fe-H	Fe-CNO	Fe-AgBr	Fe-Em
1	2.35±0.17	3.00±0.13	3.24±0.09	3.03±0.06
2	1.17±0.11	1.61±0.10	1.75±0.07	1.62±0.05
3	0.06±0.03	0.11±0.02	0.17±0.02	0.13±0.01
4		0.08±0.02	0.06±0.01	0.06±0.01
5	0.02±0.01	0.05±0.01	0.05±0.01	0.04±0.01
6		0.04±0.01	0.06±0.01	0.04±0.01
7		0.04±0.01	0.06±0.01	0.05±0.01
8		0.04±0.01	0.04±0.01	0.04±0.01
9–26	0.98±0.01	0.64±0.03	0.26±0.02	0.49±0.02

those in table 1 while the value $\langle n_{9-25} \rangle = 0.4$ estimated for Fe-AgBr reactions is larger than that obtained in this experiment.

In fig. 2 we show the multiplicity distributions of fragments with $Z = 1$ and 2. Multiplicities $n > 1$ for heavier fragments are very rare. For $Z = 3$ and 4 we observe the percentage $W(n_{Z=3,4} > 1) = 3.2\%$. For $Z = 5$–8 we found $W(n_{Z=5-8} > 1) = 1.3\%$ while no events are registered with $n_{Z \geq 9} > 1$. The average multiplicity of fragments

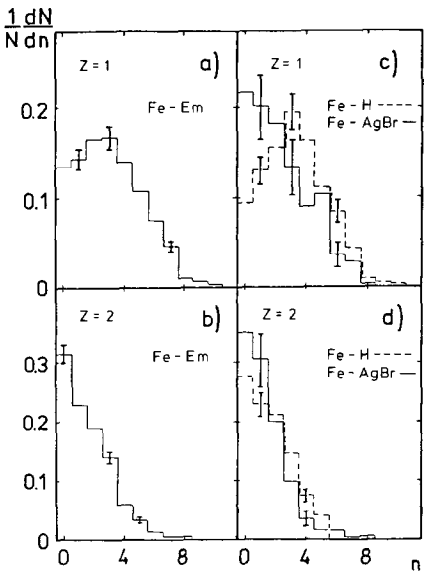

Fig. 2. Multiplicity distributions of singly ((a), (c)) and doubly ((d), (b)) charged fragments in (a), (b) Fe-Em interactions, and (c), (d) Fe-H interactions (dotted histogram), and Fe-AgBr interactions (solid histogram).

with $Z<9$ in Fe-H collisions can be compared with the multiplicity of evaporation or black particles in p-Em collisions at a primary momentum of 3.1 GeV/c [ref. [9])]. The multiplicities to be compared are $\langle n_{Z<9}\rangle$(Fe-H) $=3.60\pm0.23$ and $\langle n_b\rangle$ (p-Em) $=3.83\pm0.11$. Taking into account that at these energies $\langle n_b\rangle \sim A^{\alpha}$, where α is 0.56 ± 0.03 [ref. [9])] and A is the target mass in p-A collisions, one estimates $\langle n_b\rangle$(p-Fe) ≈ 3.5. Thus, we conclude that the average multiplicity of fragments in events classified as Fe-H collisions is in good agreement with that of the target multiplicity in p-Fe interactions.

Inclusive experiments in which forward-emitted ($\theta<0.7°$) fragments of light nuclei were detected with a spectrometer[6,10,11]) observed that fragmentation cross sections could be factorized; $\sigma^{F}_{PT}=\gamma^{F}_{P}\gamma_T$, where the designations P, T, F belong to the projectile, target and fragment, respectively. In other words, the charge composition does not depend on the target nucleus. The target factor γ_T depends weakly on A_T,

$$\gamma_T \sim A_T^{1/4}. \tag{4}$$

In 4π experiments, where the total fragmentation cross sections are measured, the exact factorization is found to be invalid. In table 2 we present some examples

TABLE 2

Charge composition of projectile fragments in interactions of ^{14}N and ^{56}Fe ions with nuclei of emulsion

Ratio of multiplicities	Projectile nucleus	Target-nucleus		
		H	CNO	AgBr
$\frac{\langle n_{Z=2}\rangle}{\langle n_{Z=1}\rangle}$	^{14}N	0.90 ± 0.07	0.78 ± 0.04	0.61 ± 0.04
$\frac{\langle n_{Z=2}\rangle}{\langle n_{Z=1}\rangle}$	^{56}Fe	0.50 ± 0.06	0.54 ± 0.04	0.54 ± 0.03
$\frac{\langle n_{Z\geq3}\rangle}{\langle n_{Z=2}\rangle}$	^{14}N	0.31 ± 0.04	0.29 ± 0.03	0.20 ± 0.04
$\frac{\langle n_{Z\geq9}\rangle}{\langle n_{Z=2}\rangle}$	^{56}Fe	0.84 ± 0.01	0.40 ± 0.02	0.15 ± 0.01

illustrating the dependence of multiplicity ratios on the mass number of the target nucleus. Table 3 compares the values of the multiplicity ratio $\langle n_Z\rangle_{AgBr}/\langle n_Z\rangle_{CNO}$ for fragmentation of iron and nitrogen nuclei. Note that the data on fragmentation of ^{14}N nuclei [12]) were obtained at $p_0=2.9$ GeV/c per nucleon. The experimental conditions were identical to those of the present experiment.

The following can be concluded:

(i) In contrast to fragmentation of ^{14}N nuclei, where multiplicities of fragments with any Z decrease with increasing A_T, multiplicities of light ($Z\leq8$) fragments

TABLE 3

The ratio of the average multiplicities of projectile fragments produced on heavy and light nuclei of emulsion

Charge of fragments Z	$\langle n_Z \rangle_{AgBr}/\langle n_Z \rangle_{CNO}$	
	^{56}Fe	^{14}N
1	1.1 ± 0.05	0.73 ± 0.04
2	1.1 ± 0.08	0.57 ± 0.04
3–4	1.2 ± 0.1	0.39 ± 0.08
5–8	1.2 ± 0.1	
≥9	0.41 ± 0.03	

from ^{56}Fe nuclei increase with the target mass number (table 1). Only the multiplicity of heavy residual fragments of iron nuclei decreases with increasing A_T. Note also that the increase of multiplicities of light fragments (cf. table 1) does not satisfy eq. (4) which gives ratios independent of the target mass.

(ii) The composition of fragments from nitrogen nuclei depends considerably on A_T for any Z-value (cf. table 3), thus showing that the factorization is broken in interactions of ^{14}N nuclei in emulsion [see also ref. [12])]. The composition of fragments is the same within experimental uncertainties for all ensembles of Fe events (Fe-H, Fe-CNO, Fe-AgBr) again with the exception for the case of heavy fragments.

Thus, the factorization of fragmentation cross sections observed at zero angle has probably a restricted region of applicability. It is broken for the integrated cross sections and the deviation from simple fragmentation increases with the mass of the incident nucleus. We show below (sect. 5) that the emission of projectile fragments in interactions induced by relativistic ^{56}Fe nuclei are quite different from the fragmentation of light nuclei (like N) and can only partially be explained by Fermi motion.

4. Transverse momentum distributions

Much information about the dynamics of the fragmentation process can be obtained from analysis of momentum distributions of fragments. An important result found in previous experiments is that the momentum components of a fragment have approximately a universal (gaussian) shape in the rest frame of the fragmenting nucleus [6]). The dispersion of this distribution has a parabolic dependence on the mass of the fragment [6]). These regularities follow naturally from the statistical approach to the fragmentation process with minimal correlations between momenta of intranuclear nucleons.

However, in 4π experiments [mainly emulsion experiments – see e.g. refs. [12,14,15])] it is observed that transverse momentum distributions of fragments can have large $p_\perp$ tails, indicating the existence of a non-statistical contribution. The contribution

of these high $p_\perp$ tails is comparatively small for the fragmentation of light (^{16}O) projectiles, except in interactions where only one light ($Z=2$–3) fragment is emitted [14]).

In the present section, we compare fragmentation of ^{56}Fe nuclei with ^{14}N and ^{12}C nuclei in emulsion at 2.9 and 4.5 GeV/c per nucleon, respectively [12,15]). Note that all the experimental data considered were obtained and processed under the same experimental conditions, except for the beam momentum.

In all cases the transverse momentum of a fragment was calculated on the basis of its emission angle

$$p_\perp = A_F p_0 \sin\theta . \tag{5}$$

It has been shown in refs. [12,15]) that for $Z=1$ the values of $p_\perp$ calculated from eq. (5) agree well with those obtained on the basis of momentum measurements. For $Z \geq 2$ we make the assumption that the mass number of the fragment A_F is $2Z$. Due to the general excess of neutron-rich isotopes for $Z \geq 3$ [see e.g. review in ref. [16])] eq. (5) gives a lower limit for the average transverse momentum.

In table 4 we present the average values of transverse momenta of fragments in ^{14}N-Em, ^{12}C-Em and ^{56}Fe-Em interactions. The most obvious feature of these data

TABLE 4

Average transverse momenta of projectile fragments in interactions of relativistic nuclei in emulsion

Charge of fragments Z	$\langle p_\perp \rangle$ (GeV/c)		
	^{12}C-Em [ref. [15])]	^{14}N-Em [ref. [12])]	^{56}Fe-Em
1	0.13 ± 0.01	0.12 ± 0.01	0.14 ± 0.01
2	0.24 ± 0.01	0.24 ± 0.01	0.37 ± 0.01
3	0.29 ± 0.02	0.24 ± 0.02	0.42 ± 0.03
4	0.23 ± 0.02	0.29 ± 0.02	0.51 ± 0.04
5	0.27 ± 0.04	0.25 ± 0.02	0.51 ± 0.06
6	0.27 ± 0.05	0.33 ± 0.03	0.53 ± 0.06
7		0.33 ± 0.09	0.60 ± 0.06
8			0.53 ± 0.05
≥9			0.52 [a])

[a]) A crude estimate based on the angular distribution of fragments with $Z \geq 9$ and the data of ref. [3]) on Z-distributions of fragments with $Z \geq 13$.

is the considerable rise of the average transverse momentum for all Z-values when comparing ^{12}C and ^{14}N with ^{56}Fe reactions. Assuming that in the range $12 \leq A_P \leq 56$, $\langle p_\perp \rangle$ can be parametrized as $\langle p_\perp \rangle \sim A_P^\alpha$, one obtains $\alpha = 0.25 \pm 0.03$ for fragments with $Z=2$ and $0.3 \leq \alpha \leq 0.5$ for heavier fragments. For singly charged fragments we can unfortunately determine only the lower limits of $\langle p_\perp \rangle$ due to the use of an

a priori postulated spectrum (1). If one uses this spectrum (1) also for identified fragments with $Z \geq 2$, i.e. when neglecting the "tails" of $p_\perp$ distributions (see below), one obtains $\langle p_\perp \rangle$ values which are significantly lower than those listed in table 4.

Note also that the neutron excess of the fragments (i.e. when $A_F > 2Z_F$) can only strengthen the observed rise of $\langle p_\perp \rangle$ in Fe-Em interactions in comparison with collisions of light projectiles.

The effect discussed here was observed first in cosmic-ray reactions more than 25 years ago [1]) – mostly for α-particles. Recently it has also been observed and discussed in an accelerator experiment, when comparing the angular distributions of α-particles in ^{56}Fe-Em and ^{16}O-Em collisions [4]).

In table 5 we show the values of $\langle p_\perp \rangle$ in interactions of ^{56}Fe ions with different target nuclei. The data exhibit a rise of $\langle p_\perp \rangle$ with the mass of the target. Using again the power approximation $\langle p_\perp \rangle \sim A_T^\beta$ one obtains $\beta \simeq 0.05$, i.e. a much weaker dependence on A_T than on A_P.

TABLE 5

Average transverse momenta of fragments in different ensembles of Fe-Em interactions

Charge of fragments Z	$\langle p_\perp \rangle$ (GeV/c)		
	Fe-H	Fe-CNO	Fe-AgBr
2	0.31 ± 0.02	0.35 ± 0.01	0.39 ± 0.01
3–4	0.42 ± 0.06	0.47 ± 0.04	0.44 ± 0.03
5–8	0.43 ± 0.10	0.51 ± 0.05	0.57 ± 0.04
≥ 9 [a])	0.49	0.52	0.56

[a]) A crude estimate (see table 4).

Transverse momentum distributions of fragments with different charges are shown in figs. 3–5. In fig. 3 we compare $p_\perp$ distributions of fragments in interactions of different projectile nuclei in emulsion. The corresponding distributions in interactions of ^{56}Fe ions with different components of emulsion are shown in fig. 4. Fig. 5 compares the $p_\perp$ distributions of fragments with $Z = 2$ and $3 \leq Z \leq 4$ with the universal gaussian distribution (eq. (2) with $\sigma = (\frac{1}{2}\langle p_\perp^2 \rangle)^{1/2}$) which corresponds to the statistical mechanism of fragmentation. Distributions for fragments with $Z = 1$ are shown in figs. 3 and 4 only for the completeness; one should remember that they are based on formula (2) thus *a priori* excluding high values of $p_\perp$.

The following can be concluded from these data:

(i) $p_\perp$ distributions for fragments with $Z \geq 2$ in Fe-Em interactions are shifted considerably towards large $p_\perp$ values in comparison to corresponding distributions for light projectile nuclei.

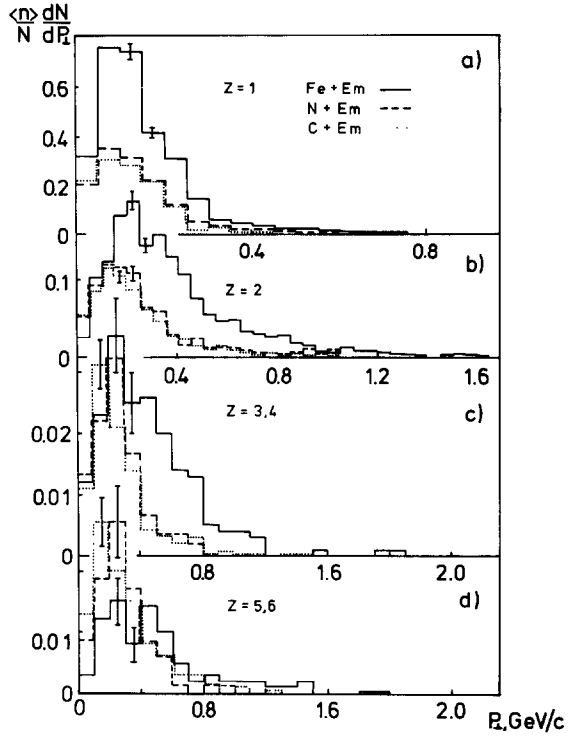

Fig. 3. Transverse momentum distributions of fragments with $Z=1$ (a), 2 (b), 3–4 (c) and 5–6 (d) in ^{12}C-Em, ^{14}N-Em and ^{56}Fe-Em collisions (the dotted, dashed and solid histogram, respectively).

(ii) The $p_\perp$ distributions depend weakly on A_T (fig. 4 and table 5). It should be noticed that even in Fe-H collisions the $p_\perp$ distributions differ from those in collisions of light projectile nuclei (see also tables 4 and 5). Thus the features of fragmentation are more dependent on the mass number of the fragmenting nucleus than the partner nucleus.

(iii) $p_\perp$ distributions for fragments of all charges cannot be well described by a simple gaussian function (cf. fig. 5). The well-known parabolic dependence of the widths of the momentum distributions on the charge of fragments remain approximately valid also in Fe-Em interactions. In fig. 6 we show the dependence of $\langle p_\perp \rangle$ (note that $\langle p_\perp \rangle = \sqrt{\frac{1}{2}\pi}\sigma$) on Z for $2 \leq Z \leq 8$ in Fe-Em collisions. It is seen that this dependence can be described by a function

$$\sigma^2 = \sigma_0^2 2Z(A_P - 2Z)/(A_P - 1)\,, \tag{6}$$

but only if σ_0 is large ($\sigma_0 = 140$ MeV/c). If one formally uses the known relations of the Fermi gas model [13]), $\sigma_0 = \frac{1}{3}\langle p^2 \rangle$ and $\langle p^2 \rangle = \frac{3}{5}p_F^2$ ($\langle p^2 \rangle$ is the mean square momentum of uncorrelated nucleons in a nucleus and p_F the Fermi momentum), the values of p_F obtained from the experimental data ($p_F \approx 0.32$ GeV/c) come out to be too high.

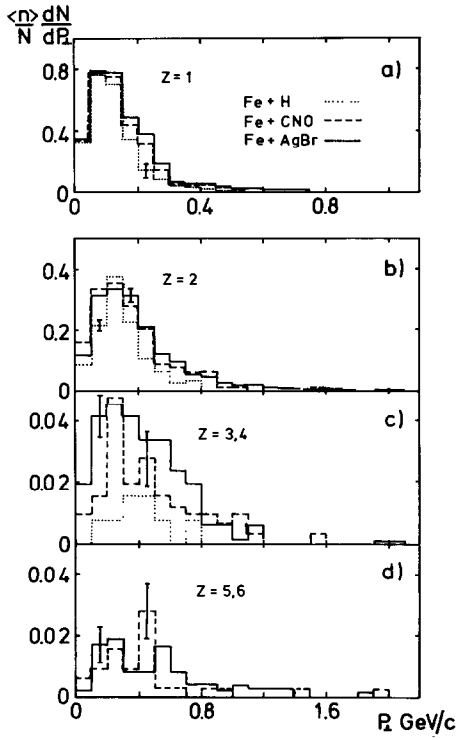

Fig. 4. The same as in fig. 3, but for Fe-H (dotted), Fe-CNO (dashed) and Fe-AgBr (solid histogram) collisions.

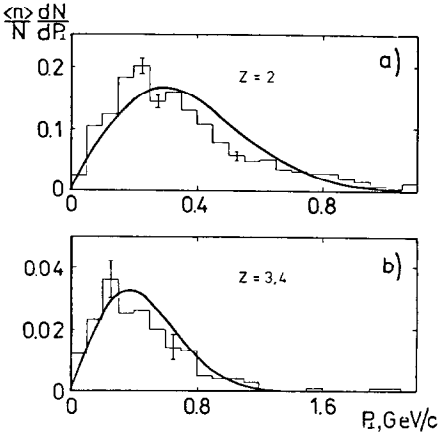

Fig. 5. A comparison between experimental $p_\perp$ distributions for fragments with $Z=2$ (a) and 3-4 (b) and a gaussian distribution eq. (6).

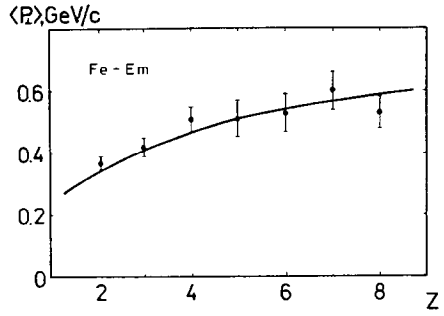

Fig. 6. $\langle p_\perp \rangle$ as a function of Z in Fe-Fm collisions. The curve exhibits the parabolic dependence described by eq. (7).

5. Azimuthal correlations

One reason for the large average transverse momentum of fragments could be that a momentum transfer to the residual nucleus is taking place prior to the fragmentation. A transverse motion of the fragmenting residue should lead to an azimuthal asymmetry of the fragmentation products.

In order to study azimuthal correlations between fragments we studied the following quantities:

(a) The azimuthal asymmetry parameter,

$$A = \left(\int_{\pi/2}^{\pi} f(\varepsilon)\, \mathrm{d}\varepsilon - \int_{0}^{\pi/2} f(\varepsilon)\, \mathrm{d}\varepsilon \right) \Big/ \int_{0}^{\pi} f(\varepsilon)\, \mathrm{d}\varepsilon , \tag{7}$$

of the inclusive distribution $(f(\varepsilon) = (1/\sigma)\, \mathrm{d}\sigma/\mathrm{d}\varepsilon$. The angle we study is $\varepsilon \equiv \varepsilon_{ij} = \arccos[(\boldsymbol{p}_{\perp i} \cdot \boldsymbol{p}_{\perp j})/|\boldsymbol{p}_{\perp i} \cdot \boldsymbol{p}_{\perp j}|]$, i.e. the angle between the transverse momenta of the ith and the jth fragment from an event $(0 \leqslant \varepsilon \leqslant \pi)$.

(b) The average value of the coefficient of azimuthal asymmetry in individual events momentum.

$$\langle \alpha \rangle = \sum_{k=1}^{N} \alpha_k / N, \qquad \alpha_k = \sum_{i=1}^{n_k - 1} \sum_{j=i+1}^{n_k} \cos \varepsilon_{ij} \sqrt{n_k (n_k - 1)}\,, \tag{8}$$

where $k = 1, 2, \ldots, N$; N being the number of events in the ensemble with a multiplicity $n_k \geqslant 2$ of fragments of considered type.

Let us recall some useful properties of eqs. (7) and (8), for the proceeding analysis:

(i) Under the assumptions of uncorrelated emission of fragments and isotropy of fragment angular distributions the ε_{ij} distribution is uniform in the interval $[0, \pi]$ and the average values of A and $\langle \alpha \rangle$ are equal to zero.

(ii) Local momentum conservation within the fragmenting nucleus (limited multiplicity) will however lead to an excess at large angles in the ε_{ij} distribution and thus $A > 0$ and $\langle \alpha \rangle < 0$.

(iii) If the decaying "fireball" has a transverse momentum this would lead to a decrease of A and an increase of $\langle\alpha\rangle$ in contrast to the local momentum conservation. The ε-distribution reveals in this case a tendency to have a maximum at $\varepsilon = 0$.

Let us now consider the experimental data. In fig. 7 we show ε_{ij} and α_k distributions for fragments with $Z \geq 2$ in Fe-Em interactions. Values of A and $\langle\alpha\rangle$ in different ensembles of collisions are listed in table 6. One can conclude from these data, that:

(i) The transverse momentum distributions of fragments are asymmetrical in the azimuthal plane. This fact indicates that the fragmenting nucleus has a transverse momentum.

(ii) The azimuthal asymmetry of fragments increases with the mass number of the target.

The latter statement follows from the data of table 6. We see from table 6 that A and $\langle\alpha\rangle$ are equal to zero in Fe-H collisions. This does not mean that projectile

TABLE 6

Coefficients of azimuthal asymmetry in different ensembles of Fe-Em collisions

Ensemble of events	A	$\langle\alpha\rangle$
Fe-H	-0.07 ± 0.06	0.00 ± 0.11
Fe-CNO	-0.10 ± 0.03	0.24 ± 0.07
Fe-AgBr	-0.15 ± 0.03	0.32 ± 0.06
Fe-Em	-0.12 ± 0.02	0.25 ± 0.04

fragments in Fe-H collisions are not correlated in the azimuthal plane. In fact, under reasonable assumptions about the total multiplicity of fragments (see below), the transverse momentum conservation alone produces expectation values of A and $\langle\alpha\rangle$ in Fe-H interactions of $A = 0.2$ and $\langle\alpha\rangle = -0.4$.

We have performed Monte Carlo calculations for Fe break-up in the picture of a fragmentation model, based on the following assumptions:

(i) The residual nucleus decays according to the cylindrical phase-space model (CPS) into n_1 singly charged, n_2 with $Z = 2$, n_3 multiply charged ($Z \geq 3$) and n_0 neutral fragments. Here the fragments are produced according to the phase-space integral with a separable transverse part of the form [19,20])

$$\frac{\mathrm{d}\sigma^{(n)}}{\mathrm{d}p_{\perp 1} \cdots \mathrm{d}p_{\perp n}} = \prod_{i=1}^{n} \Phi(p_{\perp i}) \delta^{(n)}\left(\sum_{i=1}^{n} p_{\perp i}\right) \tag{9}$$

(n is the total number of fragments, $\Phi(p_{\perp i})$ is the "cut-off" function, which takes into account that the transverse momenta of fragments are restricted).

(ii) The transverse momenta of the fragments are distributed according to eq. (2). $\langle p_\perp \rangle$ values for fragments with $Z = 1, 2, \geq 3$ are taken from table 4 (values from ^{12}C-Em and ^{14}N-Em are used) and furthermore we assume $\langle p_\perp \rangle_{Z=0} = \langle p_\perp \rangle_{Z=1}$.

(iii) The fragmenting nucleus has a transverse momentum, $\boldsymbol{p}_\perp^A$, superimposed on the "internal" transverse momenta of fragments. $|\boldsymbol{p}_\perp^A|$ was considered as an adjustable parameter.

When performing the calculations we use (table 1) $n_1 = 3$. It is assumed that the number of protons among singly charged fragments multiplied by $(A-Z)/Z$ for ^{56}Fe is equal to the number of neutrons (n_0), $n_3 = 1$ and $n_2 = 2$ or 3 (the average number of α-particles in events with $n_{Z\geq 2} \geq 2$ is equal to 2.5).

The most serious assumption here is the choice of σ (or $\langle p_\perp \rangle$) values which should characterize the internal Fermi motion of the nucleons within the fragmenting nucleus. It is reasonable to use the empirical values from fragmentation of light nuclei rather than to apply some speculative assumptions. It is, however, necessary to remember that the empirical values of $\langle p_\perp \rangle$ and σ in fragmentation of light nuclei are much larger than expected from Fermi motion alone because (a) the possible nonstatistical contribution of high $p_\perp$ tails, and (b) in fragmentation of light nuclei there may also exist a transverse motion of the residue which increase $\langle p_\perp \rangle$ just as in the case of ^{56}Fe fragmentation. On the other hand, the fragmentation of the Fe nucleus is expected to give larger $\sigma(\langle p_\perp \rangle)$ than fragmentation of light nuclei.

The main results of our calculations are presented in figs. 7–9. The following conclusions can be drawn:

(i) The presence of a transverse momentum $\boldsymbol{p}_\perp^A$ ensures the azimuthal asymmetry of fragments. All the quantitative characteristics of azimuthal asymmetry for fragments with $Z \geq 2$ in Fe-Em interactions – the average values A and $\langle \alpha \rangle$ (fig. 8), ε_{ij} and α_k distributions (fig. 7) – can be described reasonably well by the model with a transverse momentum of the fragmenting residual nucleus of $|\boldsymbol{p}_\perp^A| =$

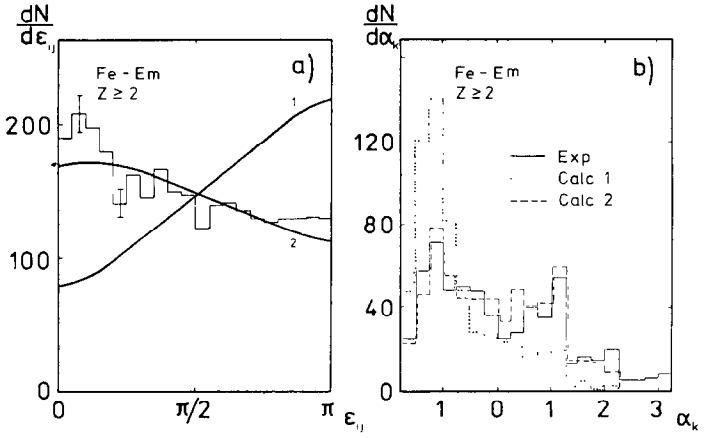

Fig. 7. Distributions of quantities ε_{ij} (a) and α_k (b) in Fe-Em collisions for fragments with $Z \leq 2$. The solid histogram exhibits experimental data. Curve 1 and dotted histogram represent the cylindrical phase-space model (CPSM) calculations (see text) with $|\boldsymbol{p}_\perp^A| = 0$, while curve 2 and the dashed histogram correspond to the CPSM with $|\boldsymbol{p}_\perp^A| = 0.15$ GeV/c.

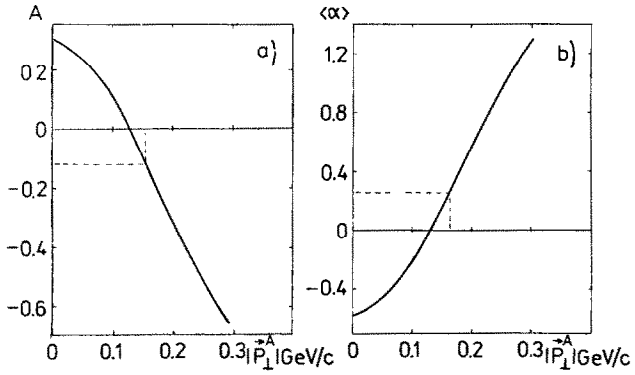

Fig. 8. Predictions of the CPSM for the dependence of A (a) and $\langle\alpha\rangle$ (b) on $|\boldsymbol{p}_\perp^A|$ for fragments with $Z \geq 2$.

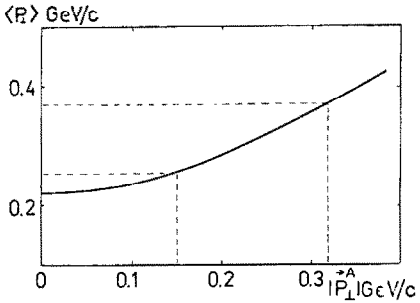

Fig. 9. Dependence of $\langle p_\perp\rangle$ for fragments with $Z<2$ on $|\boldsymbol{p}_\perp^A|$ calculated from the CPSM described in the text.

0.15 ± 0.01 GeV/c. It is necessary to point out that if we decrease the "input" values of $\langle p_\perp\rangle$ (and σ) for projectile fragments, then the magnitude of $|\boldsymbol{p}_\perp^A|$ would decrease.

(ii) In order to describe the observed large average transverse momenta of fragments from ^{56}Fe in comparison to the "input" values of $\langle p_\perp\rangle$, it is necessary to have considerably higher values of $|\boldsymbol{p}_\perp^A|$. In fig. 9 we see that for fragments with $Z=2$ (α-particles) the $|\boldsymbol{p}_\perp^A|$ value needed is 0.32 ± 0.02 GeV/c. It is important to notice that if one decreases the "input" values of $\langle p_\perp\rangle$, the corresponding value of $|\boldsymbol{p}_\perp^A|$, describing the experimental data on transverse momenta of fragments would increase. In other words, the values of the transverse momentum of the fragmenting residual nucleus, describing the observed azimuthal asymmetry, can explain only a small part (~20–30%, see fig. 9) of the increase of $\langle p_\perp\rangle$ with increasing mass of the projectile nucleus.

Finally, it should be pointed out that our calculated $\langle p_\perp\rangle - |\boldsymbol{p}_\perp^A|$ relation depends rather weakly on the assumptions of the multiplicities of fragments of different types in Fe-Em interactions.

6. Discussion and conclusions

Let us briefly summarize the main experimental observations of the present investigation and formulate the conclusions which can be drawn:

(i) Transverse momentum distributions of fragments have tails of large $p_\perp$, which cannot be described by a simple statistical model of fragmentation with no correlations between intranuclear nucleons.

(ii) The transverse momenta of projectile fragments have a strong dependence on the mass number of the projectile nucleus and a weaker dependence on the mass of the target. The mean transverse momentum of the fragments increases with increasing A_P and A_T.

(iii) The emission of fragments is asymmetrical in the azimuthal plane, which could mean that the fragmenting residual nucleus gets a transverse momentum during the collision process.

(iv) A transverse momentum of the fragmenting nucleus can, however, be responsible only for a minor part of the A_P dependence observed for the mean transverse momentum of the fragments. The main part must therefore be attributed to the dynamics of nucleus–nucleus interactions and/or structure effects.

Qualitatively, the observed effects may be due to multiple rescattering, hard processes, short-range intranuclear correlations, Coulomb repulsion between clusters, collective nuclear fluid effects and so on.

On the other hand, the data allow to draw some model-independent conclusions. Our data indicate for example that the partner nucleus is not a simple spectator of the fragmentation process.

It is necessary to remember than in the present paper we have not discussed the longitudinal momentum distributions of projectile fragments which are less sensitive to the dynamics of nucleus–nucleus interactions [see e.g. ref. [18])]. Another comment concerns the projectile fragmentation as a probe of the Fermi momentum distribution. The results of the present investigation show, that the real situation is complicated and it seems that information about the internal motion cannot be obtained (in a model-independent way) from the data on transverse momentum distribution of fragments.

We are much indebted to B.A. Bondarenko for her help in this work and the allotment of the data on ^{12}C-Em interactions. The emulsion stack has been exposed by H. Heckman. His support as well as that of the BEVALAC staff is gratefully acknowledged.

References

1) C.F. Powell, P.H. Fowler and D.H. Perkins, Study of elementary particles by the photographic method (Pergamon, London, 1959)

2) V.S. Barashenkov and V.D. Toneev, Interactions of high-energy particles and atomic nuclei with nuclei (Atomizdat, Moscow, 1972)

3) G.D. Westfall *et al.*, Phys. Rev. **C19** (1979) 1309
4) K.B. Bhalla *et al.*, Nucl. Phys. **A367** (1981) 446
5) E.S. Basova *et al.*, Yad. Fiz. **34** (1981) 1524
6) D.E. Greiner *et al.*, Phys. Rev. Lett. **35** (1975) 152
7) Alma-Ata–Leningrad–Moscow–Tashkent collaboration, Yad. Fiz. **22** (1975) 736;
K.G. Gulamov *et al.*, in Multiparticle processes at high energies (Fan, Tashkent, 1976) 78
8) T. Saito, J. Phys. Soc. Japan **30** (1971) 1243
9) E.S. Basova *et al.*, Dokl. Uzb. Akad. Sci. **8** (1980) 28; **9** (1981) 31
10) H.H. Heckman *et al.*, Phys. Rev. Lett. **28** (1972) 926
11) P.J. Lindstrom *et al.*, Lawrence Berkeley Laboratory report LBL-3650 (1975)
12) A.I. Bondarenko *et al.*, Izv. Uzb. Akad. Sci. (Phys. and Math.) **2** (1979) 73
13) A.S. Goldhaber, Phys. Lett. **B53** (1974) 306
14) B. Jakobsson *et al.*, Lett. Nuovo Cim. **15** (1976) 444
15) Bucharest–Warsaw–Dubna–Kosiĉe–Leningrad–Moscow–Tashkent collaboration, Yad. Fiz. **32** (1980) 1387
16) B. Jakobsson, CRN de Strasbourg report CRN/PN 77-3 (1977)
17) S.A. Azimov and G.M. Chernov, Statistical methods in high-energy physics (Fan, Tashkent, 1970);
S.A. Azimov *et al.*, in Multiparticle processes at high energies (Fan, Tashkent, 1976) p. 120
18) T. Fujita and J. Hüfner, Nucl. Phys. **A343** (1980) 493
19) L. van Hove, Nucl. Phys. **B9** (1969) 331
20) W. Kittel *et al.*, Comp. Phys. Comm. **1** (1979) 415